doi:10.1093/brain/awv361 BRAIN 2016: 139; 495–508 | 495

BRAIN
A JOURNAL OF NEUROLOGY

# Free-water imaging in Parkinson's disease and atypical parkinsonism

**Peggy J. Planetta,[1] Edward Ofori,[1] Ofer Pasternak,[2] Roxana G. Burciu,[1] Priyank Shukla,[1] Jesse C. DeSimone,[1] Michael S. Okun,[3,4,5] Nikolaus R. McFarland[3,4] and David E. Vaillancourt[1,4,6]**

Conventional single tensor diffusion analysis models have provided mixed findings in the substantia nigra of Parkinson's disease, but recent work using a bi-tensor analysis model has shown more promising results. Using a bi-tensor model, free-water values were found to be increased in the posterior substantia nigra of Parkinson's disease compared with controls at a single site and in a multi-site cohort. Further, free-water increased longitudinally over 1 year in the posterior substantia nigra of Parkinson's disease. Here, we test the hypothesis that other parkinsonian disorders such as multiple system atrophy and progressive supranuclear palsy have elevated free-water in the substantia nigra. Equally important, however, is whether the bi-tensor diffusion model is able to detect alterations in other brain regions beyond the substantia nigra in Parkinson's disease, multiple system atrophy, and progressive supranuclear palsy and to accurately distinguish between these diseases. Free-water and free-water-corrected fractional anisotropy maps were compared across 72 individuals in the basal ganglia, midbrain, thalamus, dentate nucleus, cerebellar peduncles, cerebellar vermis and lobules V and VI, and corpus callosum. Compared with controls, free-water was increased in the anterior and posterior substantia nigra of Parkinson's disease, multiple system atrophy, and progressive supranuclear palsy. Despite no other changes in Parkinson's disease, we observed elevated free-water in all regions except the dentate nucleus, subthalamic nucleus, and corpus callosum of multiple system atrophy, and in all regions examined for progressive supranuclear palsy. Compared with controls, free-water-corrected fractional anisotropy values were increased for multiple system atrophy in the putamen and caudate, and increased for progressive supranuclear palsy in the putamen, caudate, thalamus, and vermis, and decreased in the superior cerebellar peduncle and corpus callosum. For all disease group comparisons, the support vector machine 10-fold cross-validation area under the curve was between 0.93–1.00 and there was high sensitivity and specificity. The regions and diffusion measures selected by the model varied across comparisons and are consistent with pathological studies. In conclusion, the current study used a novel bi-tensor diffusion analysis model to indicate that all forms of parkinsonism had elevated free-water in the substantia nigra. Beyond the substantia nigra, both multiple system atrophy and progressive supranuclear palsy, but not Parkinson's disease, showed a broad network of elevated free-water and altered free-water corrected fractional anisotropy that included the basal ganglia, thalamus, and cerebellum. These findings may be helpful in the differential diagnosis of parkinsonian disorders, and thereby facilitate the development and assessment of targeted therapies.

1 Department of Applied Physiology and Kinesiology, University of Florida, USA
2 Departments of Psychiatry and Radiology, Brigham and Women's Hospital, Harvard Medical School, USA
3 Center for Movement Disorders and Neurorestoration, University of Florida, USA
4 Department of Neurology, University of Florida, USA
5 Department of Neurosurgery, University of Florida, USA
6 Department of Biomedical Engineering, University of Florida, USA

Correspondence to: David E. Vaillancourt, PhD,
Department of Applied Physiology and Kinesiology,
University of Florida, PO Box 118205, Gainesville,

Received August 24, 2015. Revised October 19, 2015. Accepted October 26, 2015. Advance Access publication December 24, 2015

FL 32611-8205,
USA
E-mail: vcourt@ufl.edu

**Keywords:** Parkinson's disease; multiple system atrophy; progressive supranuclear palsy; diffusion MRI; extracellular space

**Abbreviations:** FAt = free-water-corrected fractional anisotropy; MDS-UPDRS-III = Movement Disorder Society Unified Parkinson's Disease Rating Scale part III; MSA = multiple system atrophy; PSP = progressive supranuclear palsy

# Introduction

Parkinson's disease, multiple system atrophy (MSA), and progressive supranuclear palsy (PSP) are pathologically distinct neurodegenerative disorders that can be difficult to diagnose clinically due to their overlapping motor symptoms. Diffusion MRI provides *in vivo* microstructural measures of the brain, and has emerged as a promising tool for differentiating Parkinson's disease, MSA, and PSP. In Parkinson's disease, several single tensor diffusion imaging studies have reported reduced fractional anisotropy values in the substantia nigra (Yoshikawa *et al.*, 2004; Chan *et al.*, 2007; Vaillancourt *et al.*, 2009; Péran *et al.*, 2010; Du *et al.*, 2011; Rolheiser *et al.*, 2011; Zhan *et al.*, 2011; Skorpil *et al.*, 2012). In PSP, diffusion studies using a single tensor model have reported lower fractional anisotropy values and higher axial diffusivity, radial diffusivity, mean diffusivity, and apparent diffusion coefficient in the superior cerebellar peduncle (Blain *et al.*, 2006; Nicoletti *et al.*, 2008; Knake *et al.*, 2010; Whitwell *et al.*, 2011; Saini *et al.*, 2012; Tsukamoto *et al.*, 2012; Agosta *et al.*, 2014; Tessitore *et al.*, 2014; Worker *et al.*, 2014). In MSA, studies using a single tensor model have found lower fractional anisotropy values and higher axial diffusivity, radial diffusivity, mean diffusivity, and apparent diffusion coefficient in the middle cerebellar peduncle (Shiga *et al.*, 2005; Blain *et al.*, 2006; Nicoletti *et al.*, 2006, 2013; Paviour *et al.*, 2007; Chung *et al.*, 2009; Pellecchia *et al.*, 2009; Tha *et al.*, 2010; Tsukamoto *et al.*, 2012; Worker *et al.*, 2014), lower fractional anisotropy, higher apparent diffusion coefficient, and higher trace (D) values in the putamen (Schocke *et al.*, 2004; Nicoletti *et al.*, 2006; Ito *et al.*, 2007; Köllensperger *et al.*, 2007; Chung *et al.*, 2009; Pellecchia *et al.*, 2009; Tsukamoto *et al.*, 2012; Umemura *et al.*, 2013; Cnyrim *et al.*, 2014), and higher mean diffusivity in the cerebellar hemispheres (Nicoletti *et al.*, 2013).

Recently, however, a meta-analysis questioned the utility of fractional anisotropy and mean diffusivity in the substantia nigra as markers of Parkinson's disease when the single tensor model was used (Schwarz *et al.*, 2013). A study from the Parkinson's Progressive Marker Initiative (PPMI) was not able to find differences in single tensor fractional anisotropy within the substantia nigra for Parkinson's disease compared with controls (Schuff *et al.*, 2015), whereas a study using a more advanced diffusion model found elevated free-water in the substantia nigra using a subset of the subjects from the PPMI cohort (Ofori *et al.*, 2015*a*). The presence of free-water (i.e. water molecules that are not restricted by the cellular environment and therefore do not display a directional dependence) can significantly bias diffusion indices and lead to reduced fractional anisotropy and increased mean diffusivity values (Metzler-Baddeley *et al.*, 2012). To address this issue, a bi-tensor model was introduced that separates the diffusion properties of water in brain tissue from those of water in extracellular space (Pasternak *et al.*, 2009). Using this technique, it has been shown that free-water values are increased and free-water-corrected fractional anisotropy (FAt) values are actually unchanged in the posterior substantia nigra of patients with Parkinson's disease compared with controls in a single site and multi-site cohort (Ofori *et al.*, 2015*a*). Moreover, free-water values in the posterior substantia nigra were correlated cross-sectionally with motor symptom severity (Ofori *et al.*, 2015*a*), increased longitudinally over 1 year in Parkinson's disease, and baseline free-water values of Parkinson's disease patients were found to predict the rate of motor symptom progression over the subsequent year (Ofori *et al.*, 2015*b*). These findings suggest that there is an increase in the extracellular space of the substantia nigra in Parkinson's disease, and that free-water values using the bi-tensor model may be a more sensitive and reliable marker of Parkinson's disease and its progression than conventional diffusion measures that rely upon a single tensor model. Given that overlapping motor symptoms are clinical hallmarks of Parkinson's disease, MSA, PSP, and all show loss of dopaminergic cells at pathology in the substantia nigra region, we test the hypothesis that MSA and PSP will have elevated free-water in the substantia nigra. Equally important is whether free-water imaging is able to detect alterations in the tissue and/or extracellular space of other brain regions beyond the substantia nigra region in Parkinson's disease, MSA, and PSP, which could improve differential diagnosis. Because atypical parkinsonian syndromes typically present with a more complex clinical profile, we expected substantially more regions of altered free-water in MSA and PSP as compared to Parkinson's disease.

To this end, we compared free-water and FAt values in multiple brain regions as derived by diffusion MRI and the bi-tensor model between Parkinson's disease, MSA and PSP, and healthy age-matched controls. Regions of interest were selected based on previous pathology and neuroimaging findings in these patients (Hofer and Frahm, 2006; Ito *et al.*, 2008; Zrinzo *et al.*, 2008; Erbetta *et al.*, 2009;

**Table 1 Group demographic and clinical characteristics**

| Variable | PD | MSA | PSP | Control |
|---|---|---|---|---|
| Subjects, *n* | 18 | 18 | 18 | 18 |
| Male/female, *n* | 12/6 | 11/7 | 6/12 | 6/12 |
| Age, years | 67.9 ± 6.1 | 68.8 ± 7.6 | 69.5 ± 4.7 | 66.9 ± 6.6 |
| MDS-UPDRS-III total | 37.3 ± 6.6 | 54.1 ± 16.9 | 43.7 ± 16.7 | 2.8 ± 2.0 |
| MDS-UPDRS-III gait | 2.6 ± 1.7 | 10.5 ± 5.0 | 8.9 ± 5.5 | 0.1 ± 0.3 |
| MoCA | 25.7 ± 2.2 | 20.2 ± 5.3 | 19.2 ± 4.4 | 27.1 ± 2.0 |

MoCA = Montreal Cognitive Assessment; PD = Parkinson's disease. Data shown are sums or mean ± SD.

Dickson, 2012; Nicoletti *et al.*, 2013; Prodoehl *et al.*, 2013), and spanned the basal ganglia, midbrain, thalamus, brainstem, cerebellum, and corpus callosum. We also assessed how well free-water and FAt measures alone, and in combination with clinical measures, can distinguish the groups. For this we used logistic regression and support vector machine classification techniques.

# Materials and methods

## Participants and assessments

Seventy-two individuals participated in this study: 18 patients with Parkinson's disease, 18 patients with MSA, 18 patients with PSP, and 18 healthy age-matched controls (Table 1). Ten Parkinson's disease and nine control subjects also participated in a previous study of free-water imaging in Parkinson's disease (Ofori *et al.*, 2015*b*). All patients were diagnosed as probable by a fellowship-trained movement disorders neurologist using established criteria (Hughes *et al.*, 1992; Litvan *et al.*, 1996; Gilman *et al.*, 2008). Notably, as shown by the disease duration (Table 1), the diagnosis remained stable for >3 years. None of the control participants reported a history of neuropsychiatric or neurological problems. Research evaluations were conducted between 9:00 am and 3:00 pm, and the patients were tested following overnight withdrawal from anti-parkinsonian medications. All participants were administered the Movement Disorder Society Unified Parkinson's Disease Rating Scale part III (MDS-UPDRS-III) to evaluate motor symptom severity and the Montreal Cognitive Assessment (MoCA) to assess global cognitive functioning (Nasreddine *et al.*, 2005). An additional composite score was calculated based on items 9–13 of the MDS-UPDRS-III (MDS-UPDRS-III gait and posture, Table 1). The study was approved by the Institutional Review Board at the University of Florida. Informed written consent was obtained from each subject prior to testing.

## MRI data acquisition

All images were collected using a 3.0 T MR scanner (Philips Achieva) and 32-channel quadrature volume head coil. Head movement was minimized by foam padding within the coil and scanner noise was attenuated using a combination of earplugs and circumaural headphones. The parameters of the diffusion imaging acquisition sequence were as follows: gradient directions = 64, b-values = 0/1000 s/mm$^2$, repetition time = 7748 ms, echo time = 86 ms, flip angle = 90°, field of view = 224 × 224 mm, matrix size = 112 × 112, number of contiguous axial slices = 60, slice thickness = 2 mm, and SENSE factor $P = 2$.

## Diffusion imaging data analysis

Data preprocessing and analysis were consistent with previous work (Pasternak *et al.*, 2009; Ofori *et al.*, 2015*a*, *b*). First, we used the FMRIB Software Library (FSL; Oxford, UK) and custom UNIX shell scripts to correct for signal distortions due to eddy currents and head motion, compensate the diffusion gradients for these rotations, and remove non-brain tissues. Next, free-water and FAt maps were calculated from the preprocessed data using custom code written in MATLAB (version R2013a; The Mathworks, Natick, MA). To create the free-water map, a minimization procedure was used that fit a bi-tensor model to each voxel to quantify its fractional volume of free-water. The free-water component was then eliminated from each voxel to generate the FAt map. To standardize the data, the b-zero image of each subject was registered to a $T_2$-weighted image in MNI space (2 × 2 × 2 mm) by an affine transformation with 12 degrees of freedom and trilinear interpolation using FLIRT (http://fsl.fmrib.ox.ac.uk/fsl/fslwiki/FLIRT). The resultant transformation matrix was then applied to the free-water and FAt maps.

## Regions of interest

Regions of interest were hand-drawn on the b-zero image of each subject in MNI space by an experienced rater who was blind to group membership (Fig. 1), and then used to extract values from the corresponding free-water and FAt maps. The size of each region of interest was chosen to fit within the brain structure across all subjects. Bilateral regions of interest were drawn in the following areas (number of voxels per hemisphere, *n*): anterior substantia nigra ($n = 8$), posterior substantia nigra ($n = 8$), putamen ($n = 88$), caudate nucleus ($n = 68$), globus pallidus ($n = 76$), subthalamic nucleus ($n = 8$), red nucleus ($n = 8$), thalamus ($n = 36$), pedunculopontine nucleus ($n = 8$), dentate nucleus ($n = 20$), middle cerebellar peduncle ($n = 16$), superior cerebellar peduncle ($n = 14$), cerebellar lobule V ($n = 68$), and cerebellar lobule VI ($n = 125$). Midline regions of interest (number of voxels, *n*) were drawn in the cerebellar vermis ($n = 42$), and areas CC1 ($n = 90$) and CC2 ($n = 78$) of the corpus callosum. The cerebellar vermis region of interest was comprised of areas VIIIa, VIIIb, and IX. Note that the corpus callosum was not captured in the diffusion scan of one MSA subject because the patient was kyphotic. These missing values were replaced by the group averages prior to analysis. To assess interrater reliability, a novice rater who was blind to group membership drew all of the regions of interest on 12 subjects (three randomly selected from each group).

## Control regions of interest

To determine the sensitivity of free-water imaging in detecting disease-specific differences, we also included two control regions of interest in regions of the brain where structural changes in these diseases have not been reported (i.e. parietal

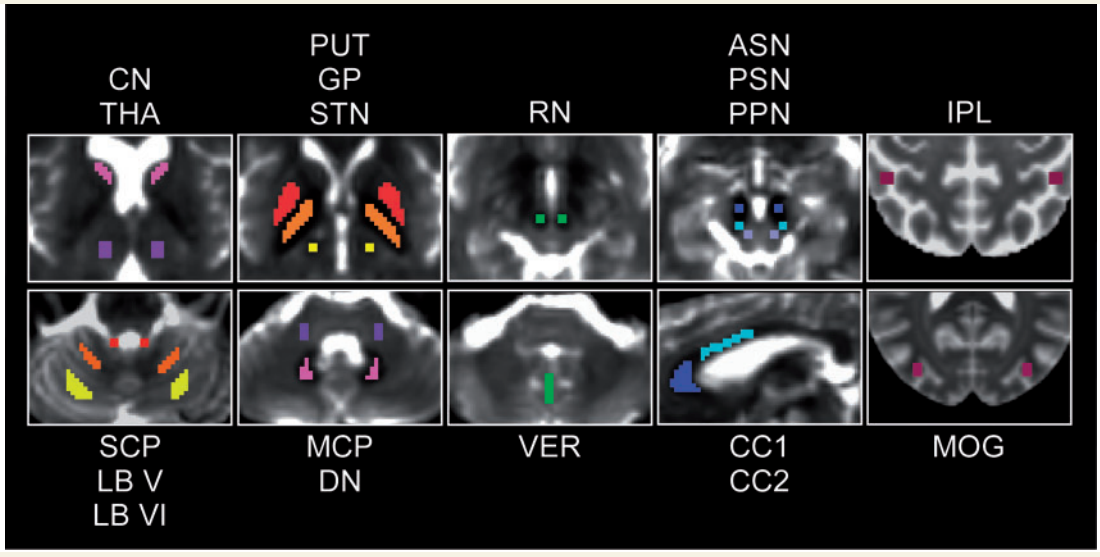


**Figure 1 Regions of interest and control regions of interest.** ASN = anterior substantia nigra; CC1 = corpus callosum region 1; CC2 = corpus callosum region 2; CN = caudate nucleus; DN = dentate nucleus; GP = globus pallidus; IPL = inferior parietal lobule; LB V = cerebellar lobule V; LB VI = cerebellar lobule VI; MCP = middle cerebellar peduncle; MOG = middle occipital gyrus; PPN = pedunculopontine nucleus; PSN = posterior substantia nigra; PUT = putamen; RN = red nucleus; SCP = superior cerebellar peduncle; STN = subthalamic nucleus; THA = thalamus; VER = vermis.

and occipital cortices). The control regions of interest were generated using a 4-mm radius and placed bilaterally in the inferior parietal lobule (IPL; MNI coordinates: $x = \pm 47$, $y = -42$, $z = 54$) and middle occipital gyrus (MOG; MNI coordinates: $x = \pm 34$, $y = -81$, $z = 20$) (Fig. 1).

## Statistical analyses

Statistical analyses were performed in SPSS (version 22.0; IBM Corp). Alpha was set at 0.05 for all tests, and corrected for multiple comparisons. Sex distribution among the groups was compared using a $\chi^2$ test. For each dependent variable we tested the homogeneity of group variances using Levene's test. Depending on the results of the Levene's test, group differences were analysed using either parametric analyses of variance or non-parametric analysis of variance (i.e. Welch's ANOVA). Where Welch's ANOVA was used, the adjusted *F*-values and within-groups degrees of freedom are reported. Free-water and FAt measures were analysed separately using a multivariate analysis of variance with sex as covariate (MANCOVA model). As 19 tests were performed per diffusion imaging measure, the alpha level was adjusted for multiple comparisons using the Bonferroni method, such that results were considered significant when *P*-values $< 0.0026$ (0.05/19). The significant group differences were followed by Bonferroni corrected pairwise comparisons. An intraclass correlation coefficient (ICC) was calculated for diffusion imaging variables (hand-drawn regions of interest) using a two-way mixed model with absolute agreement. Finally, sensitivity and specificity analyses were performed to test the accuracy of diffusion measures in classifying groups. The classification analyses based on free-water and FAt measures proceeded in two steps. The first step consisted in performing receiver operating characteristic (ROC) analyses and binary logistic regressions (forward selection method) on the diffusion imaging variables that differed significantly between groups to assess how well they could distinguish Parkinson's disease/PSP/MSA from control, PSP/MSA from Parkinson's disease, PSP from MSA, PSP from Parkinson's disease, and MSA from Parkinson's disease. In Step 2, we entered the variables selected by Step 1 into a support vector machine classification analysis using 10-fold cross-validation using the Library for Support Vector Machines (LIBSVM) (Chang and Lin, 2011). To examine the effect of clinical measures (i.e. total MDS-UPDRS-III, MDS-UPDRS-III gait and posture, and Montreal Cognitive Assessment) on the classification results, we performed two additional support vector machine analyses: one that included diffusion measures as well as clinical measures, and another one that included only clinical measures. MDS-UPDRS-III scores and Montreal Cognitive Assessment were normalized before being entered in the support vector machine analyses. Finally, we assessed the relation between the diffusion measures included in the support vector machine analysis based on the results of the logistic regression and disease severity (total MDS-UPDRS-III), and cognitive status (Montreal Cognitive Assessment) using Pearson's correlation. Correlations were performed separately for Parkinson's disease, MSA, PSP, as well as across groups. *P*-values were adjusted for multiple comparisons using the Bonferroni method (*P*-values $< 0.0045$, Bonferroni: 0.05/11).

# Results

## Demographic and clinical data

Table 1 shows the clinical and demographic data. Neither sex distribution [$\chi^2(3,72) = 6.84$, $P = 0.077$] nor age [$F(3,68) = 0.57$, $P = 0.636$] differed significantly between

groups. Disease duration did not differ significantly between patients groups [$F(2,51) = 1.93$, $P = 0.155$]. There was a significant between-group difference on the Montreal Cognitive Assessment [Welch's $F(3,35.93) = 20.86$, $P < 0.001$]. *Post hoc* tests revealed that PSP and MSA had lower scores compared with controls and Parkinson's disease ($P$-values $\leqslant 0.003$), but PSP did not differ from MSA ($P = 0.926$) and Parkinson's disease did not differ from controls ($P = 0.216$). The patient groups differed significantly on the MDS-UPDRS-III [Welch's $F(2,28.13) = 8.08$, $P = 0.002$]; MSA had higher scores than Parkinson's disease ($P = 0.002$), but PSP did not differ significantly from MSA or Parkinson's disease ($P$-values $\geqslant 0.164$). The gait and posture subscore from MDS-UPDRS-III also differed between groups [Welch's $F(2,26.63) = 27.46$, $P < 0.001$], with MSA and PSP having more severe gait and posture problems than Parkinson's disease ($P$-values $< 0.001$), and no differences between MSA and PSP ($P = 0.634$).

## Diffusion analyses

ICC values revealed excellent agreement between the two raters (Supplementary Table 1). Across all regions of interest, the intraclass correlation coefficient of average free-water values ranged from 0.951 to 0.995 (all $P$-values $< 0.001$) and ICC of average FAt values ranged from 0.947 to 0.998 (all $P$-values $< 0.001$).

Tables 2 and 3 show the mean free-water and FAt values for each region of interest by group, as well as the results of the pairwise comparisons. Free-water values differed significantly between groups in each region of interest (all $P$-values $\leqslant 0.001$), except for the control regions of interest (inferior parietal lobule, $P = 0.511$; middle occipital gyrus, $P = 791$). Compared with controls, free-water values were increased in the anterior and posterior substantia nigra of Parkinson's disease (both $P$-values $\leqslant 0.018$), most regions of interest of MSA (all $P$-values $\leqslant 0.022$ except the dentate nucleus, subthalamic nucleus, and CC2 where $P$-values $\geqslant 0.086$), and all regions of interest of PSP (all $P$-values $\leqslant 0.045$) (Fig. 2). FAt values differed significantly between groups in six regions of interest (all $P$-values $\leqslant 0.001$) (Fig. 3). The middle cerebellar peduncle $F$-value between groups was at $P = 0.006$, and approached significance. Parkinson's disease and controls did not differ in any of the regions of interest (all $P$-values $\geqslant 0.176$). MSA had increased FAt values in the caudate and putamen compared with controls (both $P$-values $< 0.001$) (Fig. 3). In PSP, FAt values were increased in the caudate, putamen, thalamus, and vermis and decreased in the superior cerebellar peduncle and CC2 compared with controls (all $P$-values $\leqslant 0.031$) (Fig. 3). No significant group differences were detected in FAt values in the two controls regions of interest (inferior parietal lobule, $P = 0.246$; middle occipital gyrus, $P = 0.722$).

## Differentiation of patients and controls

Table 4 summarizes the results of three classification models using diffusion measures alone, clinical measures alone, and a combination of diffusion and clinical measures. The classification analysis based on diffusion measures included two steps. In Step 1 using the logistic regression approach, the area under the curve was 0.97 (sensitivity 94%, specificity 89%) for control versus Parkinson's disease/MSA/PSP and 1.00 for each of the disease group comparisons (sensitivity 100%, specificity 100%). In Step 2, using the support vector machine with 10-fold cross-validation, the areas under the curve were between 0.93 and 1.00 for each comparison with strong sensitivity and specificity in each comparison (Table 4). The support vector machine with 10-fold cross-validation based on the clinical measures yielded an area under the curve of 0.99 for controls versus Parkinson's disease/MSA/PSP (sensitivity 89%, specificity 98%), an area under the curve between 0.83 and 0.95 with high sensitivity and moderate to high specificity for Parkinson's disease versus MSA/PSP, Parkinson's disease versus MSA, Parkinson's disease versus PSP, and an area under the curve of 0.50 with low sensitivity and low specificity for MSA versus PSP (Table 4). Finally, the support vector machine model based on diffusion and clinical measures provided an area under the curve of 1.00, with 100% sensitivity and 100% specificity for the comparison of controls versus Parkinson's disease/MSA/PSP, and an area under the curve between 0.88 and 1.00 for the comparisons between patients, and high sensitivity and specificity for each of these comparisons.

## Correlation of diffusion and clinical measures

Within-group correlation analyses revealed no significant association between the diffusion measures used in the classification analysis and total MDS-UPDRS-III, or Montreal Cognitive Assessment ($P$-values $> 0.05$). A negative correlation between free-water in the posterior substantia nigra and Montreal Cognitive Assessment approached significance in Parkinson's disease; however it did not survive a Bonferroni correction ($r = -0.609$, $P = 0.007$ and Bonferroni $P = 0.0045$). Across groups (Parkinson's disease/MSA/PSP, $n = 54$), total MDS-UPDRS-III was found to correlate positively with free-water from lobule V of the cerebellum ($r = 0.463$, $P < 0.001$), FAt values from putamen ($r = 0.556$, $P < 0.001$), and vermis ($r = 0.424$, $P = 0.001$). Montreal Cognitive Assessment was related to free-water in the superior cerebellar peduncle ($r = -0.509$, $P < 0.001$), and FAt in the CC2 area of the corpus callosum ($r = 0.399$, $P = 0.003$).

# Discussion

The current study is the first to use a bi-tensor model to examine free-water and FAt in the basal ganglia,

**Table 2 Free-water values for each region of interest by group**

| ROI | PD | MSA | PSP | Control |
|---|---|---|---|---|
| ASN | 0.204 ± 0.037[a] | 0.195 ± 0.031[a] | 0.235 ± 0.055[a] | 0.164 ± 0.030[b,c,d] |
| PSN | 0.215 ± 0.036[a,d] | 0.220 ± 0.028[a,d] | 0.295 ± 0.069[a,b,c] | 0.162 ± 0.025[b,c,d] |
| PUT | 0.156 ± 0.025[c] | 0.195 ± 0.044[a,b] | 0.198 ± 0.067[a] | 0.138 ± 0.016[c,d] |
| CN | 0.165 ± 0.026[c,d] | 0.200 ± 0.047[a,b] | 0.206 ± 0.043[a,b] | 0.158 ± 0.016[c,d] |
| GP | 0.154 ± 0.030[d] | 0.190 ± 0.068[a] | 0.207 ± 0.049[a,b] | 0.136 ± 0.018[c,d] |
| STN | 0.104 ± 0.015[d] | 0.106 ± 0.015[d] | 0.158 ± 0.021[a,b,c] | 0.095 ± 0.016[d] |
| RN | 0.097 ± 0.017[c,d] | 0.128 ± 0.041[a,b,d] | 0.180 ± 0.052[a,b,c] | 0.092 ± 0.015[c,d] |
| THA | 0.151 ± 0.023[c,d] | 0.188 ± 0.048[a,b] | 0.209 ± 0.043[a,b] | 0.145 ± 0.019[c,d] |
| PPN | 0.131 ± 0.022[d] | 0.151 ± 0.024[a,d] | 0.224 ± 0.033[a,b,c] | 0.119 ± 0.018[c,d] |
| DN | 0.111 ± 0.018[d] | 0.155 ± 0.070 | 0.167 ± 0.046[a,b] | 0.112 ± 0.013[d] |
| MCP | 0.071 ± 0.011[c] | 0.150 ± 0.101[a,b] | 0.085 ± 0.019[a] | 0.072 ± 0.008[c,d] |
| SCP | 0.320 ± 0.069[c,d] | 0.475 ± 0.119[a,b,d] | 0.664 ± 0.100[a,b,c] | 0.317 ± 0.052[c,d] |
| VER | 0.146 ± 0.030 | 0.176 ± 0.035[a] | 0.157 ± 0.024[a] | 0.135 ± 0.019[c,d] |
| LB V | 0.137 ± 0.007[c,d] | 0.208 ± 0.056[a,b] | 0.174 ± 0.025[a,b] | 0.137 ± 0.017[c,d] |
| LB VI | 0.130 ± 0.009[c,d] | 0.167 ± 0.046[a,b] | 0.145 ± 0.017[a,b] | 0.124 ± 0.016[c,d] |
| CC1 | 0.208 ± 0.045[d] | 0.248 ± 0.059[a] | 0.256 ± 0.049[a,b] | 0.199 ± 0.036[c,d] |
| CC2 | 0.310 ± 0.065[d] | 0.339 ± 0.080[d] | 0.427 ± 0.062[a,b,c] | 0.286 ± 0.044[d] |
| IPL | 0.687 ± 0.171 | 0.582 ± 0.257 | 0.634 ± 0.186 | 0.595 ± 0.195 |
| MOG | 0.323 ± 0.104 | 0.312 ± 0.108 | 0.352 ± 0.087 | 0.301 ± 0.112 |

ASN = anterior substantia nigra; CC1 = corpus callosum region 1; CC2 = corpus callosum region 2; CN = caudate nucleus; DN = dentate nucleus; GP = globus pallidus; IPL = inferior parietal lobe; LB V = cerebellar lobule V; LB VI = cerebellar lobule VI; MCP = middle cerebellar peduncle; MOG = middle occipital gyrus; PD = Parkinson's disease; PPN = pedunculopontine nucleus; PSN = posterior substantia nigra; PUT = putamen; ROI = region of interest; RN = red nucleus; SCP = superior cerebellar peduncle; STN = subthalamic nucleus; THA = thalamus; VER = vermis. Data shown are mean ± SD. $P < 0.05$ (corrected) [a]versus Control, [b]versus Parkinson's disease, [c]versus MSA, [d]versus PSP.

**Table 3 Free-water-corrected fractional anisotropy values for each region of interest by group**

| ROI | PD | MSA | PSP | Control |
|---|---|---|---|---|
| ASN | 0.628 ± 0.060 | 0.611 ± 0.061 | 0.650 ± 0.060 | 0.617 ± 0.066 |
| PSN | 0.607 ± 0.061 | 0.633 ± 0.033 | 0.643 ± 0.063 | 0.587 ± 0.068 |
| PUT | 0.219 ± 0.042[c] | 0.273 ± 0.051[a,b] | 0.237 ± 0.024[a] | 0.203 ± 0.032[c,d] |
| CN | 0.215 ± 0.028[c,d] | 0.257 ± 0.048[a,b] | 0.252 ± 0.032[a,b] | 0.203 ± 0.032[c,d] |
| GP | 0.383 ± 0.027 | 0.408 ± 0.037 | 0.392 ± 0.040 | 0.392 ± 0.042 |
| STN | 0.523 ± 0.049 | 0.539 ± 0.037 | 0.569 ± 0.041 | 0.538 ± 0.039 |
| RN | 0.540 ± 0.057 | 0.548 ± 0.074 | 0.569 ± 0.049 | 0.550 ± 0.045 |
| THA | 0.341 ± 0.021[d] | 0.351 ± 0.029[d] | 0.396 ± 0.029[a,b,c] | 0.332 ± 0.028[d] |
| PPN | 0.532 ± 0.043 | 0.523 ± 0.048 | 0.561 ± 0.060 | 0.542 ± 0.045 |
| DN | 0.400 ± 0.047 | 0.397 ± 0.057 | 0.385 ± 0.052 | 0.393 ± 0.062 |
| MCP | 0.727 ± 0.042 | 0.711 ± 0.057 | 0.754 ± 0.051 | 0.699 ± 0.039 |
| SCP | 0.730 ± 0.061[d] | 0.731 ± 0.048[d] | 0.617 ± 0.083[a,b,c] | 0.751 ± 0.031[d] |
| VER | 0.247 ± 0.028[c,d] | 0.302 ± 0.051[b] | 0.304 ± 0.040[a,b] | 0.263 ± 0.037[d] |
| LB V | 0.253 ± 0.023 | 0.254 ± 0.018 | 0.243 ± 0.017 | 0.248 ± 0.019 |
| LB VI | 0.254 ± 0.018 | 0.235 ± 0.024 | 0.238 ± 0.016 | 0.242 ± 0.017 |
| CC1 | 0.827 ± 0.028 | 0.817 ± 0.031 | 0.813 ± 0.033 | 0.823 ± 0.029 |
| CC2 | 0.764 ± 0.029[d] | 0.732 ± 0.046 | 0.698 ± 0.046[a,b] | 0.765 ± 0.028[d] |
| IPL | 0.132 ± 0.057 | 0.167 ± 0.771 | 0.140 ± 0.052 | 0.160 ± 0.049 |
| MOG | 0.228 ± 0.064 | 0.235 ± 0.052 | 0.223 ± 0.044 | 0.214 ± 0.056 |

ASN = anterior substantia nigra; CC1 = corpus callosum region 1; CC2 = corpus callosum region 2; CN = caudate nucleus; DN = dentate nucleus; GP = globus pallidus; IPL = inferior parietal lobe; LB V = cerebellar lobule V; LB VI = cerebellar lobule VI; MCP = middle cerebellar peduncle; MOG = middle occipital gyrus; PD = Parkinson's disease; PPN = pedunculopontine nucleus; PSN = posterior substantia nigra; PUT = putamen; RN = red nucleus; ROI = region of interest; SCP = superior cerebellar peduncle; STN = subthalamic nucleus; THA = thalamus; VER = vermis. Data shown are mean ± SD. $P < 0.05$ (corrected) [a]versus Control, [b]versus Parkinson's disease, [c]versus MSA, [d]versus PSP.

midbrain, thalamus, cerebellum, and corpus callosum of Parkinson's disease, MSA, PSP, and healthy controls. There were three key findings. First, we found evidence that supported the hypothesis that free-water is elevated in the substantia nigra of MSA and PSP when compared with controls, and reconfirmed the finding that free-water in the substantia nigra is elevated in Parkinson's disease compared with controls. Second, despite no other changes

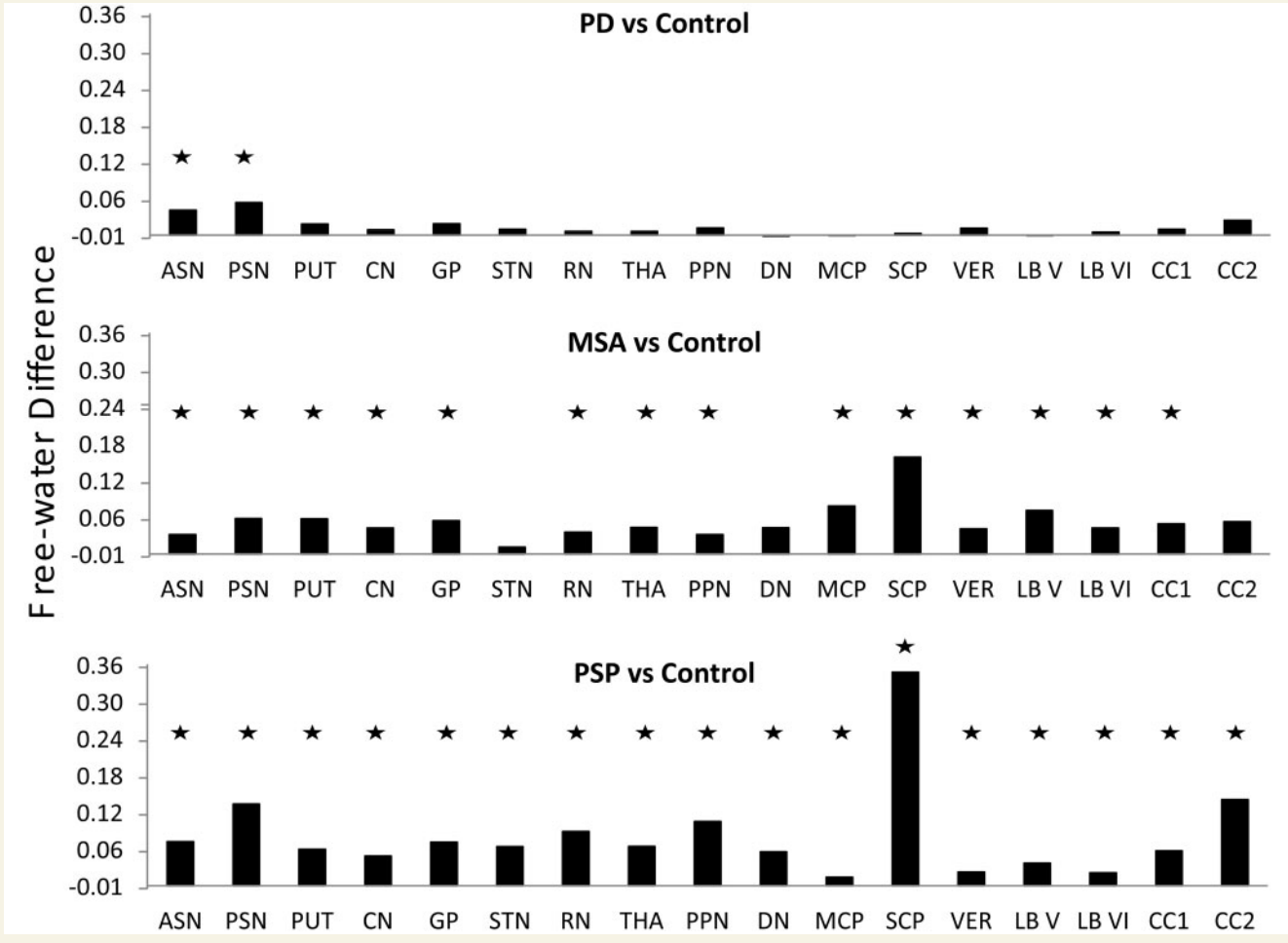


**Figure 2 Mean difference in free-water values in each region of interest for Parkinson's disease-control (*top*), MSA-control (*middle*), and PSP-control (*bottom*).** ASN = anterior substantia nigra; CC1 = corpus callosum region 1; CC2 = corpus callosum region 2; CN = caudate nucleus; DN = dentate nucleus; GP = globus pallidus; LB V = cerebellar lobule V; LB VI = cerebellar lobule VI; MCP = middle cerebellar peduncle; MSA = multiple system atrophy; PD = Parkinson's disease; PPN = pedunculopontine nucleus; PSN = posterior substantia nigra; PSP = progressive supranuclear palsy; PUT = putamen; RN = red nucleus; SCP = superior cerebellar peduncle; STN = subthalamic nucleus; THA = thalamus; VER = vermis. Asterisks denote a significant difference after correction for multiple comparisons.

in free-water or FAt for Parkinson's disease, we observed elevated free-water in multiple basal ganglia and cerebellar regions for MSA, and in all regions except for the control regions for PSP. Compared with controls, FAt was increased for MSA in the putamen and caudate, and increased for PSP in the putamen, caudate, thalamus, and vermis, and decreased in the superior cerebellar peduncle and corpus callosum. These findings, along with the fact that no group differences were detected in the control regions within parietal and occipital cortices, suggest that the bi-tensor model is sensitive to disease-specific alterations, and provides clear patterns and distinct differences across the brain in Parkinson's disease, MSA, and PSP (Figs 2 and 3). Third, when combining free-water and FAt values from multiple regions that are consistent with prior pathology studies in each disease, the cross-validated machine learning algorithm separated the disease groups with excellent sensitivity and specificity (Table 4).

The pathological hallmarks of Parkinson's disease are the loss of dopaminergic neurons in the substantia nigra (Fearnley and Lees, 1991) and presence of Lewy bodies and Lewy neurites (Braak *et al.*, 2003). The current findings of elevated free-water in the posterior substantia nigra of the Parkinson's disease group confirms prior work (Ofori *et al.*, 2015*a*, *b*), and extends the elevated substantia nigra free-water to MSA and PSP. FAt in the substantia nigra was not different for any of the groups compared with controls, suggesting that prior studies examining the substantia nigra using a single tensor model were due to free-water. Further, we observed increased free-water in the anterior substantia nigra of Parkinson's disease, MSA, and PSP, when compared with controls. In prior work (Ofori *et al.*, 2015*a*, *b*), a significant increase in free-water for the

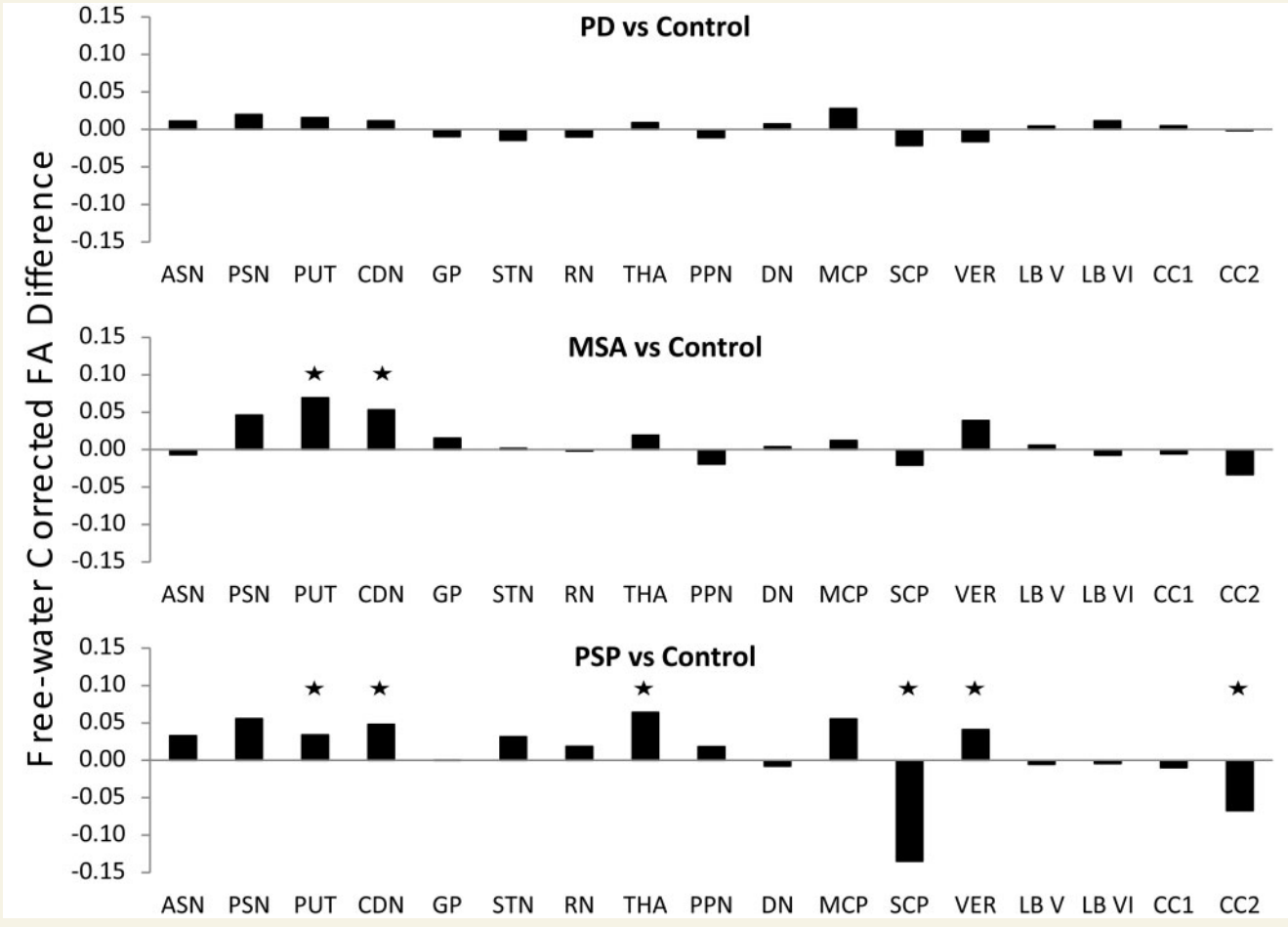


**Figure 3 Mean difference in free-water-corrected fractional anisotropy values in each region of interest for Parkinson's disease-control (*top*), MSA-control (*middle*), and PSP-control (*bottom*).** ASN = anterior substantia nigra; CC2 = corpus callosum region 2; CN = caudate nucleus; LB VI = cerebellar lobule VI; MCP = middle cerebellar peduncle; MSA = multiple system atrophy; PD = Parkinson's disease; PSN = posterior substantia nigra; PSP = progressive supranuclear palsy; PUT = putamen; SCP = superior cerebellar peduncle; STN = subthalamic nucleus; THA = thalamus; VER = vermis. Asterisks denote a significant difference after correction for multiple comparisons.

anterior substantia nigra region was not observed for early stage Parkinson's disease, and the difference in results in the anterior substantia nigra between the current study and prior work is likely due to the differences in the disease severity of the patients. The current study included Parkinson's disease with more severe motor symptoms (MDS-UPDRS-III OFF medication = 37.3), whereas the cross-sectional study by Ofori and colleagues (2015*a*) included an early stage cohort (MDS-UPDRS III OFF medication = 29.8) and a drug-naïve cohort (MDS-UPDRS-III OFF medication = 22.9) with milder levels of disease severity. As in the current study free-water in the anterior substantia nigra was also impaired in the MSA and PSP cohorts, it could be that as the disease spreads and becomes more severe the anterior substantia nigra free-water values are more likely to become affected. In support of this hypothesis, a cross-sectional study of disease progression in Parkinson's disease found that fractional anisotropy values in the anterior substantia nigra were altered only in the later stages of disease (Du *et al.*, 2012).

Consistent with several other diffusion MRI studies, we did not observe significant differences in diffusivity in areas beyond the substantia nigra in Parkinson's disease compared with controls (Seppi *et al.*, 2003; Schocke *et al.*, 2004; Blain *et al.*, 2006; Rizzo *et al.*, 2008; Boelmans *et al.*, 2010; Nicoletti *et al.*, 2010, 2013; Wang *et al.*, 2010; Tsukamoto *et al.*, 2012; Worker *et al.*, 2014). Nevertheless, altered diffusion has been reported in a variety of areas that differ across studies, including the basal ganglia, thalamus (Péran *et al.*, 2010; Zhan *et al.*, 2011; Kim *et al.*, 2013), corpus callosum (Karagulle Kendi *et al.*, 2008; Gattellaro *et al.*, 2009), cerebral cortex (Nicoletti *et al.*, 2006; Karagulle Kendi *et al.*, 2008; Zhan *et al.*, 2011; Zhang *et al.*, 2011), middle cerebellar peduncle (Agosta *et al.*, 2014), and cerebellar hemispheres (Zhang *et al.*, 2011; Mormina *et al.*, 2015). Differences in methodology, patient characteristics, and the potential bias of free-water on single tensor diffusion measures may explain these mixed results. Our results also raise the possibility that those Parkinson's disease studies that detected

**Table 4 Summary of the three group classification models**

| Comparison<br>Diffusion MRI measures | AUC | Sens | Spec | |
|---|---|---|---|---|
| **Step 1 Binary logistic regression** | | | | **Variables selected by logistic regression model** |
| CON versus PD/MSA/PSP | 0.97 | 94 | 89 | PSN (FW), SCP (FAt) |
| PD versus MSA/PSP | 1.00 | 100 | 100 | SCP (FW), SCP (FAt), PUT (FAt), VER (FAt), CC2 (FAt) |
| PD versus MSA | 1.00 | 100 | 100 | THA (FW), LB V (FW), CN (FAt) |
| PD versus PSP | 1.00 | 100 | 100 | SCP (FW) |
| MSA versus PSP | 1.00 | 100 | 100 | PPN (FW), STN (FW) |
| **Step 2 Support vector machine** | | | | **Variables entered based on model in Step 1** |
| CON versus PD/MSA/PSP | 0.93 | 94 | 83 | PSN (FW), SCP (FAt) |
| PD versus MSA/PSP | 0.94 | 93 | 89 | SCP (FW), SCP (FAt), PUT (FAt), VER (FAt), CC2 (FAt) |
| PD versus MSA | 0.97 | 95 | 89 | THA (FW), LB V (FW), CN (FAt) |
| PD versus PSP | 1.00 | 100 | 100 | SCP (FW) |
| MSA versus PSP | 0.97 | 95 | 94 | PPN (FW), STN (FW) |
| **Clinical measures** | | | | |
| **Support vector machine** | | | | **Variables** |
| CON versus PD/MSA/PSP | 0.99 | 89 | 98 | MDS-UPDRS-III, MDS-UPDRS-III G and P, MoCA |
| PD versus MSA/PSP | 0.94 | 94 | 80 | MDS-UPDRS-III, MDS-UPDRS-III G and P, MoCA |
| PD versus MSA | 0.83 | 94 | 72 | MDS-UPDRS-III, MDS-UPDRS-III G and P, MoCA |
| PD versus PSP | 1.00 | 100 | 100 | MDS-UPDRS-III, MDS-UPDRS-III G and P, MoCA |
| MSA versus PSP | 0.50 | 56 | 45 | MDS-UPDRS-III, MDS-UPDRS-III G and P, MoCA |
| **Diffusion MRI and clinical measures** | | | | |
| **Support vector machine** | | | | **Variables** |
| CON versus PD/MSA/PSP | 1.00 | 100 | 100 | PSN (FW), SCP (FAt), MDS-UPDRS-III, MDS-UPDRS-III G and P, MoCA |
| PD versus MSA/PSP | 0.98 | 95 | 94 | SCP (FW), SCP (FAt), PUT (FAt), VER (FAt), CC2 (FAt), MDS-UPDRS-III, MDS-UPDRS-III G and P, MoCA |
| PD versus MSA | 0.88 | 95 | 72 | THA (FW), LB V (FW), CN (FAt), MDS-UPDRS-III, MDS-UPDRS-III G and P, MoCA |
| PD versus PSP | 1.00 | 100 | 100 | SCP (FW), MDS-UPDRS-III, MDS-UPDRS-III G and P, MoCA |
| MSA versus PSP | 0.98 | 94 | 89 | PPN (FW), STN (FW), MDS-UPDRS-III, MDS-UPDRS-III G and P, MoCA |

Diffusion MRI measures: The results of the binary logistic regression and support vector machine cross-validation analysis based on diffusion measures.
Clinical measures: The results of the support vector machine analysis on clinical measures, whereas 'diffusion MRI and clinical measures' shows the results of the support vector machine analysis on diffusion and clinical measures.
AUC = area under the curve; CC2 = corpus callosum region 2; CN = caudate nucleus; FW = free water; LB V = cerebellar lobule V; MDS-UPDRS-III G and P = gait and posture subscore of the MDS-UPDRS-III; MoCA = Montreal Cognitive Assessment; PPN = pedunculopontine nucleus; PSN = posterior substantia nigra; SCP = superior cerebellar peduncle; Sens = sensitivity; Spec = specificity; STN = subthalamic nucleus; THA = thalamus; VER = vermis.

effects in other regions of the brain could have included patients with atypical forms of parkinsonism. This possibility further highlights the need to assess and corroborate different diffusion computational methods in order to maximize accuracy of diagnosis in parkinsonian disorders and outcomes in clinical trials.

MSA is characterized by widespread $\alpha$-synuclein-positive glial cytoplasmic inclusions and degeneration of the nigrostriatal and/or olivopontocerebellar systems (Trojanowski *et al.*, 2007). Indeed, pathological changes occur throughout the basal ganglia, with the substantia nigra and putamen most affected and the subthalamic nucleus (STN) least affected (Wenning *et al.*, 1997; Cykowski *et al.*, 2015; Salvesen *et al.*, 2015). Here, for the MSA group we observed increased free-water values in each of the basal ganglia nuclei except the STN, which is consistent with prior studies of pathology. In addition, FAt values were increased in the putamen and caudate, and increased fractional anisotropy in grey matter regions could be a signal of gliosis (Budde *et al.*, 2011). Although altered diffusion has been reported consistently in the putamen of MSA (Seppi *et al.*, 2003; Kanazawa *et al.*, 2004; Schocke *et al.*, 2004; Nicoletti *et al.*, 2006; Ito *et al.*, 2007; Köllensperger *et al.*, 2007; Chung *et al.*, 2009; Pellecchia *et al.*, 2009; Tsukamoto *et al.*, 2012; Baudrexel *et al.*, 2013; Umemura *et al.*, 2013; Cnyrim *et al.*, 2014), the microstructural composition of the other basal ganglia nuclei is less clear, results are more variable, and STN has not been a focus of previous research. Correlation analyses revealed a significant positive relation across disease groups between total MDS-UPDRS-III and FAt values in the putamen, lobule V of the cerebellum, and cerebellar vermis. Previous diffusion MRI work in MSA has reported normal (Kanazawa *et al.*, 2004; Tsukamoto *et al.*, 2012) and increased regional apparent diffusion coefficient values in the thalamus (Nicoletti *et al.*, 2006), but has not examined the red or pedunculopontine nuclei. We found increased free-water values in each of these areas. Although the red nucleus,

pedunculopontine, and thalamic nuclei are considered to be spared or only mildly affected in MSA (Dickson, 2012), there is evidence of glial cytoplasmic and neuronal inclusions in the thalamus (Cykowski *et al.*, 2015), activated microglia in the red nucleus (Salvesen *et al.*, 2015), and severe cell loss in the pedunculopontine nucleus.

In the olivopontocerebellar system, we found increased free-water values in the middle and superior cerebellar peduncles, lobules V and VI, and vermis of MSA compared with controls. Except for the superior cerebellar peduncle, each of these areas has been reported to be pathologically affected in MSA (Papp *et al.*, 1989; Wenning *et al.*, 1997; Ozawa *et al.*, 2004; Ahmed *et al.*, 2012). It is interesting to note that only PSP had a massive reduction in the superior cerebellar peduncle for the FAt measure, suggesting that this is critical in separating PSP from MSA.

In PSP, there is extensive neuronal loss and the presence of neurofibrillary tangles and neuropil threads (Litvan *et al.*, 1996). Consistent with the severe pathology throughout the basal ganglia in PSP (Hardman *et al.*, 1997; Ahmed *et al.*, 2008; Dickson, 2012), we observed increased free-water in the anterior and posterior substantia nigra, putamen, caudate, globus pallidus, and subthalamic nucleus of PSP compared with controls. In addition, FAt values were increased in caudate nucleus. Although previous research has found altered diffusion in the substantia nigra of PSP (Yoshikawa *et al.*, 2004; Knake *et al.*, 2010; Wang *et al.*, 2010; Focke *et al.*, 2011*b*), the direction of these changes has not been consistent; fractional anisotropy was increased in one study (Wang *et al.*, 2010) and reduced in another (Yoshikawa *et al.*, 2004). This inconsistent pattern could be due to the ambiguity of the single tensor model, where fractional anisotropy changes are affected by free-water differences. The major contribution of the current study is the use of the bi-tensor model, which allows us to control for partial volume effects with extracellular free-water when quantifying the fractional anisotropy metric, and thus provide a corrected fractional anisotropy value that is more specific to microstructural tissue changes.

The efferent cerebellar pathway is severely affected in PSP, with significant atrophy reported in the dentate nucleus, superior cerebellar peduncle, red nucleus, and thalamus (Tsuboi *et al.*, 2003; Halliday *et al.*, 2005; Ahmed *et al.*, 2008; Kanazawa *et al.*, 2009; Dickson, 2012). Moreover, the pedunculopontine nucleus (PPN), which is connected to the basal ganglia, thalamus, and cerebellum (Muthusamy *et al.*, 2007) is also pathologically affected in PSP (Dickson, 2012). In the current study, we found increased free-water values in each of these areas and massively reduced FAt values in the superior cerebellar peduncle. Free-water values in the superior cerebellar peduncle correlated negatively with Montreal Cognitive Assessment across disease groups.

The cerebellar cortex and vermis also exhibit pathology in PSP (Piao *et al.*, 2002; Armstrong *et al.*, 2007). In the current study, free-water values were increased in the cerebellar hemispheres and vermis and increased FAt values in the vermis. Neurons in motor cortical areas project to the vermis and are thought to be involved in whole-body posture and locomotion (Coffman *et al.*, 2011), which are disrupted in PSP. One previous diffusion MRI study reported increased radial diffusivity in the vermis and increased radial diffusivity and fractional anisotropy in the cerebellar hemispheres using track-based spatial statistics (Knake *et al.*, 2010), while another reported increased mean diffusivity in the vermis but not the hemispheres using a region of interest approach (Nicoletti *et al.*, 2013). It is possible that specific subareas of the cerebellar hemispheres are affected in PSP, but these were not detected by the region of interest study because values were averaged across the whole structure. We drew regions of interest in lobules V and VI, which are known to be involved in sensorimotor processing (Stoodley and Schmahmann, 2009; Mottolese *et al.*, 2013), and found that PSP had increased free-water values in both areas. Nevertheless, it remains to be determined whether other regions of the cerebellar cortex are affected in PSP.

In the corpus callosum, PSP had increased free-water values in CC1 and CC2 and decreased FAt values in CC2. Across disease groups, FAt in CC2 correlated positively with Montreal Cognitive Assessment. Given that areas CC1 and CC2 contain interhemispheric connections between prefrontal and motor cortices, respectively (Hofer and Frahm, 2006; Fling *et al.*, 2013), these results suggest that the frontal lobes are affected in PSP, confirming cortical pathology in this population (Dickson, 2012).

Previous MRI and pathology studies have reported that the middle cerebellar peduncle is affected in MSA, whereas the superior cerebellar peduncle is affected in PSP (Papp *et al.*, 1989; Dickson, 2012). Here, we show that free-water values are increased in the middle and superior cerebellar peduncles for both MSA and PSP compared with controls and Parkinson's disease. However, PSP had a very large reduction in the FAt values in the superior cerebellar peduncle compared with all groups consistent with predictions from pathology (Dickson, 2012). Moreover, it has been shown that PSP-Richardson's syndrome but not PSP-parkinsonism patients have increased mean diffusivity and reduced fractional anisotropy and volume in the middle and superior cerebellar peduncles compared with controls (Agosta *et al.*, 2012). Taken together, these findings suggest that the afferent and efferent cerebellar pathways are affected in MSA and PSP, albeit to different extents, and that their involvement may depend in part on disease subtype.

There has been increasing interest in using MRI-derived measures to classify parkinsonian disorders. Some diffusion-weighted imaging studies have reported excellent separation of MSA from Parkinson's disease (Schocke *et al.*, 2004; Köllensperger *et al.*, 2007), MSA from both Parkinson's disease and PSP (Nicoletti *et al.*, 2006, 2013), and PSP from Parkinson's disease (Seppi *et al.*, 2003; Nicoletti *et al.*, 2008). However, none have distinguished between Parkinson's disease, MSA and PSP in the same

cohorts, which is important to achieve given that misdiagnoses occur between all three diseases (Litvan *et al.*, 1997; Hughes *et al.*, 2001, 2002). Other MRI techniques such as regional volumetry based on $T_1$-weighted images and iron imaging based on $T_2$ maps have shown discriminative potential (Focke *et al.*, 2011*a*; Boelmans *et al.*, 2012). However, these methods have not been able to produce high classification accuracy for all comparisons. Of the studies using single tensor DTI (Blain *et al.*, 2006; Focke *et al.*, 2011*b*; Prodoehl *et al.*, 2013), the best separation of Parkinson's disease, MSA, and PSP was achieved by combining diffusion measures from multiple regions of interest (100% specificity, 87–94% sensitivity) (Prodoehl *et al.*, 2013), yet this study used a single tensor approach. There is extensive variability in diffusion metrics across studies in Parkinson's disease when using a single tensor model (Schwarz *et al.*, 2013). Abnormal diffusion imaging values from the substantia nigra in Parkinson's disease (including fractional anisotropy, radial diffusivity, and axial diffusivity) were not found using a single tensor model in a large dataset of Parkinson's disease and controls from multiple imaging sites participating in the Parkinson's Progressive Marker Initiative (Schuff *et al.*, 2015). However, in a study that applied the bi-tensor model using a subset of subjects from the same Parkinson's Progressive Marker Initiative cohort, elevated free-water was found in the posterior substantia nigra (Ofori *et al.*, 2015*a*). Thus, while prior studies have shown promise using a single tensor analysis model, this approach is not as strong and reliable in the literature as a whole. The current findings are important because the data shown in Figs 2 and 3 provide clear patterns of change using free-water and FAt in Parkinson's disease, MSA, and PSP that could not be achieved using a single tensor model.

In addition, using a multi-target approach with free-water and FAt values, the current study distinguished Parkinson's disease, MSA, and PSP with >93% area under the curve when cross-validation methods were used. Importantly, the regions used in the classification model were consistent with areas that are different in prior studies of pathology (Dickson, 2012). Free-water and FAt measures also provide an accurate separation of MSA and PSP (Table 4)—separation that cannot be done on clinical measures alone (Table 4). Equally important is that the accuracy of all group classifications based on free-water and FAt measures is not reduced by differences in clinical measures. Adding differences in motor severity, gait and posture, and global cognitive function to the classification model (Table 4) provided the advantage over diffusion measures alone, that of a perfect separation of patients from controls (AUC = 1.00, 100% sensitivity and specificity). The disadvantage of adding clinical measures to classification was that the Parkinson's disease versus MSA classification dropped from an AUC of 0.97 to 0.88. Nevertheless, these data suggest that combining clinical measures and diffusion measures based on the bi-tensor diffusion model could prove to be an effective combination should these findings be replicated in the future.

There are a few limitations worth noting. First, patients were diagnosed clinically based on the established consensus criteria for each disease (Hughes *et al.*, 1992; Litvan *et al.*, 1996; Gilman *et al.*, 2008). Given that neuropathological confirmation was not available for most patients, diagnostic errors may have occurred. However, this possibility was minimized by having movement disorders neurologists diagnose the patients (Hughes *et al.*, 2002) based on successive evaluations, and then reconfirming each patient's diagnosis by a movement disorders neurologist over several years (Table 1). Second, free-water and FAt values were calculated from manually-drawn regions of interest. This approach could be criticized for being operator-dependent, yet both raters had a strong agreement (Supplementary Table 1). Also, given the small size of several brain areas known to be affected in these diseases (e.g. substantia nigra, PPN) and their variability in spatial location between subjects due to individual differences and neurodegeneration, it could be problematic to purely rely upon a voxel-wise or other automated procedure because of the inaccuracy that occurs in spatial normalization.

In conclusion, the current study revealed distinct patterns of microstructural brain changes in Parkinson's disease, MSA, and PSP. Specifically, Parkinson's disease had select changes in free-water in the substantia nigra, MSA had widespread changes in free-water and FAt, and PSP had the most severe and widespread changes in both measures. It will be up to future work to elucidate the relationship between free-water and FAt and neurodegenerative processes such as neuroinflammation, gliosis, cell loss, and axonal damage. We also showed that free-water and FAt values from multiple regions of interest were able to distinguish the disease groups with excellent sensitivity and specificity. Although an important next step will be to determine whether our findings can be replicated using different scanners and patient cohorts, the current findings provide an important step forward in developing a robust MRI procedure to separate forms of parkinsonism.

## Acknowledgements

We thank Soo Ha for assisting with data processing and the participants for their time and commitment to the research.

## Funding

This work was supported by the National Institutes of Health (R01 NS052318, R01 NS075012, T32 NS082168) and the Bachmann-Strauss Dystonia and Parkinson Foundation.

# Supplementary material

Supplementary material is available at *Brain* online.

# References


Agosta F, Galantucci S, Svetel M, Lukić MJ, Copetti M, Davidovic K, et al. Clinical, cognitive, and behavioural correlates of white matter damage in progressive supranuclear palsy. J Neurol 2014; 261: 913–24.

Agosta F, Pievani M, Svetel M, Ječmenica Lukić M, Copetti M, Tomić A, et al. Diffusion tensor MRI contributes to differentiate Richardson's syndrome from PSP-parkinsonism. Neurobiol Aging 2012; 33: 2817–26.

Ahmed Z, Asi YT, Sailer A, Lees AJ, Houlden H, Revesz T, et al. The neuropathology, pathophysiology and genetics of multiple system atrophy [Review]. Neuropathol Appl Neurobiol 2012; 38: 4–24.

Ahmed Z, Josephs KA, Gonzalez J, DelleDonne A, Dickson DW. Clinical and neuropathologic features of progressive supranuclear palsy with severe pallido-nigro-luysial degeneration and axonal dystrophy. Brain 2008; 131: 460–72.

Arai K, Braak E, De Vos RA, Jansen Steur EN, Braak H. Mossy fiber involvement in progressive supranuclear palsy. Acta Neuropathol 1999; 98: 341–4.

Armstrong RA, Lantos PL, Cairns NJ. Progressive supranuclear palsy (PSP): a quantitative study of the pathological changes in cortical and subcortical regions of eight cases. J Neural Transm 2007; 114: 1569–77.

Baudrexel S, Seifried C, Penndorf B, Klein JC, Middendorp M, Steinmetz H, et al. The value of putaminal diffusion imaging versus 18-fluorodeoxyglucose positron emission tomography for the differential diagnosis of the Parkinson variant of multiple system atrophy. Mov Disord 2013; 29: 380–7.

Blain CRV, Barker GJ, Jarosz JM, Coyle NA, Landau S, Brown RG, et al. Measuring brain stem and cerebellar damage in parkinsonian syndromes using diffusion tensor MRI. Neurology 2006; 67: 2199–205.

Boelmans K, Bodammer NC, Suchorska B, Kaufmann J, Ebersbach G, Heinze HJ, et al. Diffusion tensor imaging of the corpus callosum differentiates corticobasal syndrome from Parkinson's disease. Parkinsonism Relat Disord 2010; 16: 498–502.

Boelmans K, Holst B, Hackius M, Finsterbusch J, Gerloff C, Fiehler J, et al. Brain iron deposition fingerprints in Parkinson's disease and progressive supranuclear palsy. Mov Disord 2012; 27: 421–7.

Braak H, Del Tredici K, Rüb U, de Vos RA, Jansen Steur EN, Braak E. Staging of brain pathology related to sporadic Parkinson's disease. Neurobiol Aging 2003; 24: 197–211.

Budde MD, Janes L, Gold E, Turtzo LC, Frank JA. The contribution of gliosis to diffusion tensor anisotropy and tractography following traumatic brain injury: validation in the rat using Fourier analysis of stained tissue sections. Brain 2011; 134(Pt 8): 2248–60.

Chan LL, Rumpel H, Yap K, Lee E, Loo HV, Ho GL, et al. Case control study of diffusion tensor imaging in Parkinson's disease. J Neurol Neurosurg Psychiatry 2007; 78: 1383–6.

Chang CC, Lin CJ. LIBSVM: a library for support vector machines. ACM Trans Intell Syst Technol 2011; 2: 1–27.

Chung EJ, Kim EG, Bae JS, Eun CK, Lee KS, Oh M, et al. Usefulness of diffusion-weighted MRI for differentiation between Parkinson's disease and Parkinson variant of multiple system atrophy. J Mov Disord 2009; 2: 64–8.

Cnyrim CD, Kupsch A, Ebersbach G, Hoffmann KT. Diffusion tensor imaging in idiopathic Parkinson's disease and multisystem atrophy (Parkinsonian type). Neurodegener Dis 2014; 13: 1–8.

Coffman KA, Dum RP, Strick PL. Cerebellar vermis is a target of projections from the motor areas in the cerebral cortex. Proc Natl Acad Sci USA 2011; 108: 16068–73.

Cykowski MD, Coon EA, Powell SZ, Jenkins SM, Benarroch EE, Low PA, et al. Expanding the spectrum of neuronal pathology in multiple system atrophy. Brain 2015; 138: 2293–309. doi:10.1093/brain/awv114.

Dickson DW. Parkinson's disease and parkinsonism: neuropathology. Cold Spring Harb Perspect Med 2012; 2: pii: a009258.

Du G, Lewis MM, Sen S, Wang J, Shaffer ML, Styner M, et al. Imaging nigral pathology and clinical progression in Parkinson's disease. Mov Disord 2012; 27: 1636–43.

Du G, Lewis MM, Styner M, Shaffer ML, Sen S, Yang QX, et al. Combined R2* and diffusion tensor imaging changes in the substantia Nigra in Parkinson's disease. Mov Disord 2011; 26: 1627–32.

Erbetta A, Mandelli ML, Savoiardo M, Grisoli M, Bizzi A, Soliveri P, et al. Diffusion tensor imaging shows different topographic involvement of the thalamus in progressive supranuclear palsy and corticobasal degeneration. Am J Neuroradiol 2009; 30: 1482–7.

Fearnley JM, Lees AJ. Ageing and Parkinson's disease: substantia nigra regional selectivity. Brain 1991; 114 (Pt 5): 2283–301.

Fling BW, Benson BL, Seidler RD. Transcallosal sensorimotor fiber tract structure-function relationships. Human Brain Mapping 2013; 34: 384–95.

Focke NK, Helms G, Scheewe S, Pantel PM, Bachmann CG, Dechent P, et al. Individual voxel-based subtype prediction can differentiate progressive supranuclear palsy from idiopathic Parkinson syndrome and healthy controls. Hum Brain Mapp 2011a; 32: 1905–15.

Focke NK, Helms G, Pantel PM, Scheewe S, Knauth M, Bachmann CG, et al. Differentiation of typical and atypical parkinson syndromes by quantitative MR imaging. Am J Neuroradiol 2011b; 32: 2087–92.

Gattellaro G, Minati L, Grisoli M, Mariani C, Carella F, Osio M, et al. White matter involvement in idiopathic Parkinson disease: a diffusion tensor imaging study. Am J Neuroradiol 2009; 30: 1222–6.

Gilman S, Wenning GK, Low PA, Brooks DJ, Mathias CJ, Trojanowski JQ, et al. Second consensus statement on the diagnosis of multiple system atrophy. Neurology 2008; 71: 670–6.

Halliday GM, Macdonald V, Henderson JM. A comparison of degeneration in motor thalamus and cortex between progressive supranuclear palsy and Parkinson's disease. Brain 2005; 128: 2272–80.

Hardman CD, Halliday GM, McRitchie DA, Cartwright HR, Morris JG. Progressive supranuclear palsy affects both the substantia nigra pars compacta and reticulata. Exp Neurol 1997; 144: 183–92.

Hofer S, Frahm J. Topography of the human corpus callosum revisited–comprehensive fiber tractography using diffusion tensor magnetic resonance imaging. Neuroimage 2006; 32: 989–94.

Hughes AJ, Daniel SE, Ben-Shlomo Y, Lees AJ. The accuracy of diagnosis of parkinsonian syndromes in a specialist movement disorder service. Brain 2002; 125(Pt 4): 861–70.

Hughes AJ, Daniel SE, Kilford L, Lees AJ. Accuracy of clinical diagnosis of idiopathic Parkinson's disease: a clinico-pathological study of 100 cases. J Neurol Neurosurg Psychiatry 1992; 55: 181–4.

Hughes AJ, Daniel SE, Lees AJ. Improved accuracy of clinical diagnosis of Lewy body Parkinson's disease. Neurology 2001; 57: 1497–9.

Ito M, Watanabe H, Kawai Y, Atsuta N, Tanaka F, Naganawa S, et al. Usefulness of combined fractional anisotropy and apparent diffusion coefficient values for detection of involvement in multiple system atrophy. J Neurol Neurosurg Psychiatry 2007; 78: 722–8.

Ito S, Makino T, Shirai W, Hattori T. Diffusion tensor analysis of corpus callosum in progressive supranuclear palsy. Neuroradiology 2008; 50: 981–5.

Kanazawa M, Shimohata T, Terajima K, Onodera O, Tanaka K, Tsuji S, et al. Quantitative evaluation of brainstem involvement in multiple system atrophy by diffusion-weighted MR imaging. Journal of Neurology 2004; 251: 1121–4.

Kanazawa M, Shimohata T, Toyoshima Y, Tada M, Kakita A, Morita T, et al. Cerebellar involvement in progressive supranuclear palsy: a clinicopathological study. Mov Disord 2009; 24: 1312–8.

Karagulle Kendi AT, Lehericy S, Luciana M, Ugurbil K, Tuite P. Altered diffusion in the frontal lobe in Parkinson disease. Am J Neuroradiol 2008; 29: 501–5.

Kim HJ, Kim SJ, Kim HS, Choi CG, Kim N, Han S, et al. Alterations of mean diffusivity in brain white matter and deep gray matter in Parkinson's disease. Neuroscience Letters 2013; 550: 64–8.

Knake S, Belke M, Menzler K, Pilatus U, Eggert KM, Oertel WH, et al. *In vivo* demonstration of microstructural brain pathology in progressive supranuclear palsy: a DTI study using TBSS. Mov Disord 2010; 25: 1232–8.

Köllensperger M, Seppi K, Liener C, Boesch S, Heute D, Mair KJ, et al. Diffusion weighted imaging best discriminates PD from MSA-P: a comparison with tilt table testing and heart MIBG scintigraphy. Mov Disord 2007; 22: 1771–6.

Litvan I, Agid Y, Calne D, Campbell G, Dubois B, Duvoisin RC, et al. Clinical research criteria for the diagnosis of progressive supranuclear palsy (Steele-Richardson-Olszewski syndrome): report of the NINDS-SPSP international workshop. Neurology 1996; 47: 1–9.

Litvan I, Goetz CG, Jankovic J, Wenning GK, Booth V, Bartko JJ, et al. What is the accuracy of the clinical diagnosis of multiple system atrophy? A clinicopathologic study. Arch Neurol 1997; 54: 937–44.

Metzler-Baddeley C, O'Sullivan MJ, Bells S, Pasternak O, Jones DK. How and how not to correct for CSF-contamination in diffusion MRI. Neuroimage 2012; 59: 1394–403.

Mormina E, Arrigo A, Calamuneri A, Granata F, Quartarone A, Ghilardi MF, et al. Diffusion tensor imaging parameters' changes of cerebellar hemispheres in Parkinson's disease. Neuroradiology 2015; 57: 327–34.

Mottolese C, Richard N, Harquel S, Szathmari A, Sirigu A, Desmurget M. Mapping motor representations in the human cerebellum. Brain 2013; 136: 330–42.

Muthusamy KA, Aravamuthan BR, Kringelbach ML, Jenkinson N, Voets NL, Johansen-Berg H, et al. Connectivity of the human pedunculopontine nucleus region and diffusion tensor imaging in surgical targeting. J Neurosurg 2007; 107: 814–20.

Nasreddine ZS, Phillips NA, Bédirian V, Charbonneau S, Whitehead V, Collin I, et al. The Montreal Cognitive Assessment, MoCA: a brief screening tool for mild cognitive impairment. J Am Geriatr Soc 2005; 53: 695–9.

Nicoletti G, Lodi R, Condino F, Tonon C, Fera F, Malucelli E, et al. Apparent diffusion coefficient measurements of the middle cerebellar peduncle differentiate the Parkinson variant of MSA from Parkinson's disease and progressive supranuclear palsy. Brain 2006; 129: 2679–87.

Nicoletti G, Manners D, Novellino F, Condino F, Malucelli E, Barbiroli B, et al. Diffusion tensor MRI changes in cerebellar structures of patients with familial essential tremor. Neurology 2010; 74: 988–94.

Nicoletti G, Rizzo G, Barbagallo G, Tonon C, Condino F, Manners D, et al. Diffusivity of cerebellar hemispheres enables discrimination of cerebellar or parkinsonian multiple system atrophy from progressive supranuclear palsy–Richardson syndrome and Parkinson disease. Radiology 2013; 267: 843–50.

Nicoletti G, Tonon C, Lodi R, Condino F, Manners D, Malucelli E, et al. Apparent diffusion coefficient of the superior cerebellar peduncle differentiates progressive supranuclear palsy from Parkinson's disease. Mov Disord 2008; 23: 2370–6.

Ofori E, Pasternak O, Planetta PJ, Burciu R, Snyder A, Febo M, et al. Increased free water in the substantia nigra of Parkinson's disease: a single-site and multi-site study. Neurobiol Aging 2015a; 36: 1097–104.

Ofori E, Pasternak O, Planetta PJ, Li H, Burciu RG, Snyder AF, et al. Longitudinal changes in free-water within the substantia nigra of Parkinson's disease. Brain 2015b; 138: 2322–2331.

Ozawa T, Paviour D, Quinn NP, Josephs KA, Sangha H, Kilford L, et al. The spectrum of pathological involvement of the striatonigral and olivopontocerebellar systems in multiple system atrophy: clinicopathological correlations. Brain 2004; 127(Pt 12): 2657–71.

Papp MI, Kahn JE, Lantos PL. Glial cytoplasmic inclusions in the CNS of patients with multiple system atrophy (striatonigral degeneration, olivopontocerebellar atrophy and Shy-Drager syndrome). J Neurol Sci 1989; 94: 79–100.

Pasternak O, Sochen N, Gur Y, Intrator N, Assaf Y. Free water elimination and mapping from diffusion MRI. Magn Reson Med 2009; 62: 717–30.

Paviour DC, Thornton JS, Lees AJ, Jäger HR. Diffusion-weighted magnetic resonance imaging differentiates Parkinsonian variant of multiple-system atrophy from progressive supranuclear palsy. Mov Disord 2007; 22: 68–74.

Pellecchia MT, Barone P, Mollica C, Salvatore E, Ianniciello M, Longo K, et al. Diffusion-weighted imaging in multiple system atrophy: a comparison between clinical subtypes. Mov Disord 2009; 24: 689–96.

Péran P, Cherubini A, Assogna F, Piras F, Quattrocchi C, Peppe A, et al. Magnetic resonance imaging markers of Parkinson's disease nigrostriatal signature. Brain 2010; 133: 3423–33.

Piao YS, Hayashi S, Wakabayashi K, Kakita A, Aida I, Yamada M, et al. Cerebellar cortical tau pathology in progressive supranuclear palsy and corticobasal degeneration. Acta Neuropathol 2002; 103: 469–74.

Prodoehl J, Li H, Planetta PJ, Goetz CG, Shannon KM, Tangonan R, et al. Diffusion tensor imaging of Parkinson's disease, atypical parkinsonism, and essential tremor. Mov Disord 2013; 28: 1816–22.

Rizzo G, Martinelli P, Manners D, Scaglione C, Tonon C, Cortelli P, et al. Diffusion-weighted brain imaging study of patients with clinical diagnosis of corticobasal degeneration, progressive supranuclear palsy and Parkinson's disease. Brain 2008; 131: 2690–700.

Rolheiser TM, Fulton HG, Good KP, Fisk JD, McKelvey JR, Scherfler C, et al. Diffusion tensor imaging and olfactory identification testing in early-stage Parkinson's disease. J Neurol 2011; 258: 1254–60.

Saini J, Bagepally BS, Sandhya M, Pasha SA, Yadav R, Pal PK. *In vivo* evaluation of white matter pathology in patients of progressive supranuclear palsy using TBSS. Neuroradiology 2012; 54: 771–80.

Salvesen L, Ullerup BH, Sunay FB, Brudek T, Løkkegaard A, Agander TK, et al. Changes in total cell numbers of the basal ganglia in patients with multiple system atrophy—a stereological study. Neurobiol Dis 2015; 74: 104–13.

Schocke MF, Seppi K, Esterhammer R, Kremser C, Mair KJ, Czermak BV, et al. Trace of diffusion tensor differentiates the Parkinson variant of multiple system atrophy and Parkinson's disease. Neuroimage 2004; 21: 1443–51.

Schuff N, Wu IW, Buckley S, Foster ED, Coffey CS, Gitelman DR et al. Diffusion imaging of nigral alterations in early Parkinson's disease with dopaminergic deficits. Mov Disord 2015. Advance Access published on August 11, 2015, doi: 10.1002/mds.26325.

Schwarz ST, Abaei M, Gontu V, Morgan PS, Bajaj N, Auer DP. Diffusion tensor imaging of nigral degeneration in Parkinson's disease: a region-of-interest and voxel-based study at 3 T and systematic review with meta-analysis. Neuroimage Clin 2013; 3: 481–8.

Seppi K, Schocke MF, Esterhammer R, Kremser C, Brenneis C, Mueller J, et al. Diffusion-weighted imaging discriminates progressive supranuclear palsy from PD, but not from the parkinson variant of multiple system atrophy. Neurology 2003; 60: 922–7.

Shiga K, Yamada K, Yoshikawa K, Mizuno T, Nishimura T, Nakagawa M. Local tissue anisotropy decreases in cerebellopetal fibers and pyramidal tract in multiple system atrophy. J Neurol 2005; 252: 589–96.

Skorpil M, Söderlund V, Sundin A, Svenningsson P. MRI diffusion in Parkinson's disease: using the technique's inherent directional

information to study the olfactory bulb and substantia nigra. J Parkinsons Dis 2012; 2: 171–80.

Stoodley CJ, Schmahmann JD. Functional topography in the human cerebellum: a meta-analysis of neuroimaging studies. Neuroimage 2009; 44: 489–501.

Tessitore A, Giordano A, Caiazzo G, Corbo D, De Micco R, Russo A, et al. Clinical correlations of microstructural changes in progressive supranuclear palsy. Neurobiol Aging 2014; 35: 2404–10.

Tha KK, Terae S, Yabe I, Miyamoto T, Soma H, Zaitsu Y, et al. Microstructural white matter abnormalities of multiple system atrophy: *in vivo* topographic illustration by using diffusion-tensor MR imaging. Radiology 2010; 255: 563–9.

Trojanowski JQ, Revesz T, Msa NWGo. Proposed neuropathological criteria for the post mortem diagnosis of multiple system atrophy. Neuropathol Appl Neurobiol 2007; 33: 615–20.

Tsuboi Y, Slowinski J, Josephs KA, Honer WG, Wszolek ZK, Dickson DW. Atrophy of superior cerebellar peduncle in progressive supranuclear palsy. Neurology 2003; 60: 1766–9.

Tsukamoto K, Matsusue E, Kanasaki Y, Kakite S, Fujii S, Kaminou T, et al. Significance of apparent diffusion coefficient measurement for the differential diagnosis of multiple system atrophy, progressive supranuclear palsy, and Parkinson's disease: evaluation by 3.0-T MR imaging. Neuroradiology 2012; 54: 947–55.

Umemura A, Oeda T, Hayashi R, Tomita S, Kohsaka M, Yamamoto K, et al. Diagnostic accuracy of apparent diffusion coefficient and 123I-metaiodobenzylguanidine for differentiation of multiple system atrophy and Parkinson's disease. PLoS One 2013; 8: e61066.

Vaillancourt DE, Spraker MB, Prodoehl J, Abraham I, Corcos DM, Zhou XJ, et al. High-resolution diffusion tensor imaging in the substantia nigra of de novo Parkinson disease. Neurology 2009; 72: 1378–84.

Wang J, Wai Y, Lin WY, Ng S, Wang CH, Hsieh R, et al. Microstructural changes in patients with progressive supranuclear palsy: a diffusion tensor imaging study. J Magn Reson Imaging 2010; 32: 69–75.

Wenning GK, Tison F, Ben Shlomo Y, Daniel SE, Quinn NP. Multiple system atrophy: a review of 203 pathologically proven cases. Mov Disord 1997; 12: 133–47.

Whitwell JL, Master AV, Avula R, Kantarci K, Eggers SD, Edmonson HA, et al. Clinical correlates of white matter tract degeneration in progressive supranuclear palsy. Arch Neurol 2011; 68: 753–60.

Worker A, Blain C, Jarosz J, Chaudhuri KR, Barker GJ, Williams SC, et al. Diffusion tensor imaging of Parkinson's disease, multiple system atrophy and progressive supranuclear palsy: a tract-based spatial statistics study. PLoS One 2014; 18: e112638.

Yoshikawa K, Nakata Y, Yamada K, Nakagawa M. Early pathological changes in the parkinsonian brain demonstrated by diffusion tensor MRI. J Neurol Neurosurg Psychiatry 2004; 75: 481–4.

Zhan W, Kang GA, Glass GA, Zhang Y, Shirley C, Millin R, et al. Regional alterations of brain microstructure in parkinson's disease using diffusion tensor imaging. Mov Disord 2011; 27: 90–7.

Zhang K, Yu C, Zhang Y, Wu X, Zhu C, Chan P, et al. Voxel-based analysis of diffusion tensor indices in the brain in patients with Parkinson's disease. Eur J Radiol 2011; 77: 269–73.

Zrinzo L, Zrinzo LV, Tisch S, Limousin PD, Yousry TA, Afshar F, et al. Stereotactic localization of the human pedunculopontine nucleus: atlas-based coordinates and validation of a magnetic resonance imaging protocol for direct localization. Brain 2008; 131: 1588–98.